

MOL #61424

I κ B kinase β regulates redox homeostasis by controlling the constitutive levels of glutathione*

Zhimin Peng, Esmond Geh, Liang Chen, Qinghang Meng, Yunxia Fan, Maureen Sartor, Howard G. Shertzer, Zheng-Gang Liu, Alvaro Puga and Ying Xia

Department of Environmental Health and Center of Environmental Genetics, University of Cincinnati Medical Center, Cincinnati, OH 45267-0056, USA, (ZP, EG, LC, QM, YF, MS, HGS, AP and YX)
Cell and Cancer Biology Branch, Center for Cancer Research, National Cancer Institute, NIH, Bethesda, MD 20892, USA, (ZGL)

MOL #61424

Running Title: IKK β regulates GSH and stress toxicity

To whom correspondence should be addressed:

Ying Xia, Ph.D. Department of Environmental Health, College of Medicine, University of Cincinnati,

123 East Shields Street, Cincinnati, Ohio 45267-0056,

Phone: (513)-558-0371; FAX: (513)-558-4397; Email: ying.xia@uc.edu

Text Pages:

Figures: 6

Table: 1

References: 41

Words in Abstract: 209

Words in Introduction: 645

Words in Discussion: 642

Abbreviations:

NF- κ B, Nuclear Factor κ B, **ikB**, Inhibitor of κ B, **IKK**, ikB kinase, **GSH**, glutathione; **GCLC**,

Glutamine Cysteine Ligase Catalytic subunit; **GCLM**, Glutamine Cysteine Ligase Modifier subunit;

TNFR, Tumor Necrosis Factor Receptor; **TRAF**, TNF Receptor Associated Factor; **AP-1**, Activator

Protein-1; **NRF2**, NF-E2-Related Factor-2; **ROS**, Reactive Oxygen Species

MOL #61424

ABSTRACT

Cytokine-activated I κ B kinase β (IKK β) is a key mediator of immune and inflammatory responses, but recent studies suggest that IKK β is also required for tissue homeostasis in physio-pathological processes. Here we report a novel role for IKK β in maintenance of constitutive levels of the redox scavenger glutathione (GSH). Inactivation of IKK β by genetic or pharmacological means results in low cellular GSH content and marked reduction of redox potential. Similar to *Ikk β* (-/-) cells, *Tnfr1* (-/-) and *p65* (-/-) cells are also GSH deficient. As a consequence, cells deficient in IKK β signaling are extremely susceptible to toxicity caused by environmental and pharmacological agents, including oxidants, genotoxic agents, microtubule toxins and arsenic. GSH biosynthesis depends on the activity of the rate limiting enzyme glutamate-cysteine ligase (GCL), consisting of a catalytic (GCLC) and a modifier (GCLM) subunit. We find that loss of IKK β signaling significantly reduces basal NF- κ B activity and decreases binding of NF- κ B to the promoters of *Gclc* and *Gclm*, leading to reduction of GCLC and GCLM expression. Conversely, overexpression of GCLC and GCLM in IKK β -null cells partially restores GSH content and prevents stress-induced cytotoxicity. We suggest that maintenance of GSH is a novel physiological role of the IKK β -NF- κ B signaling cascade to prevent oxidative damage and preserve the functional integrity of the cells.

MOL #61424

INTRODUCTION

The Nuclear Factor- κ B (NF- κ B) is a stimulus-activated transcription factor involved in the control of fundamental cellular processes, such as proliferation, apoptosis and differentiation (Pahl, 1999). NF- κ B is normally sequestered by I κ B α as an inactive complex in the cytosol, but activated by growth factors and inflammatory cytokines, such as TNF α . TNF α binds to its receptor and activates a receptor-associated signalsome, composed of TRADD, TRAF2/5, RIP and MAP3Ks. The receptor complex in turn activates IKK β , which phosphorylates I κ B α followed by I κ B α ubiquitylation and proteasome-dependent degradation. Subsequently, NF- κ B is released from I κ B α and translocates to the nucleus, where it binds to consensus NF- κ B sites in DNA to activate gene expression (Pahl, 1999). Through binding to its target DNA, widely distributed in the genome, NF- κ B participates in the regulation of a vast number of genes and diverse cell activities.

Cytokine-induced activation of the IKK-NF- κ B cascade is best known for its roles in innate immunity and inflammatory responses, but emerging evidence indicates that this pathway is required for the modulation of stress responses. *In vitro* studies show that cells deficient in IKK β , IKK β upstream TRAF2 and TRAF5, or downstream NF- κ B RelA/p65 subunit, have reactive oxidative species (ROS) accumulation and are extremely sensitive to apoptosis in response to toxic compounds and stress inducers (Cosulich et al., 2000; Kamata et al., 2005; Chen et al., 2003; Peng et al., 2007; Sakon et al., 2003). *In vivo*, hepatocyte-specific IKK β deficient mice show reduced anti-oxidant expression and excessive ROS in the liver in response to diethylnitrosamine (DEN), which is metabolized into an alkylating agent that induces oxidative stresses and causes DNA damage. The ROS in turn lead to sustained activation of JUN N-terminal kinases (JNKs) and increased liver cell death (Boitier et al.,

MOL #61424

1995;Maeda et al., 2005). Cumulatively, these observations suggest that the classical IKK β -NF- κ B pathway may help to maintain cellular redox potential and prevent oxidative stress.

The thiol group-containing tripeptide L- γ -glutamyl-L-cysteinyl-L-glycine (glutathione; GSH) is a prominent intracellular antioxidant responsible for hydrophilic scavenging of radicals and for maintaining the redox state of proteins. In most cell types, GSH plays a major role in protecting cells against toxicity arising from environmental stresses (Meister and Anderson, 1983). GSH level is primarily determined by its *de novo* synthesis, carried out by the consecutive action of the two ATP-dependent enzymes glutamate cysteine ligase (GCL) and GSH synthase (GS) (Meister and Anderson, 1983). GCL is a holoenzyme, consisting of a catalytic (GCLC) and a regulatory subunit (GCLM), and acts as the rate-limiting enzyme for GSH biosynthesis. Many oxidative stress and abnormal growth conditions can induce GCLC and GCLM expression, resulting in elevated GCL activity and GSH levels. In these cases, the elevated GSH serves as a natural defense mechanism for cells to fight against stress conditions (Lu, 2008). In addition to detoxification, GSH also participates in maintaining physiological homeostasis and balance of the biological systems, whereas, its deficiency is associated with a wide range of pathological conditions, including cancer, neurological disorders and rapid aging (Townsend et al., 2003).

A number of stress-activated transcription factors, such as AP-1, NRF2 and NF- κ B, are involved in the regulation of *Gclc* and *Gclm* at the level of gene transcription (Sierra-Rivera et al., 1994;Lu, 2008). It was shown that NF- κ B can directly bind to and activate the *Gclc* promoter, while it regulates indirectly the *Gclm* promoter by activating AP-1 (Yang et al., 2005b). A dominant negative NF- κ B blocks basal and TNF α -induced expression of GCLC and GCLM, but the intracellular signaling

MOL #61424

pathways responsible for GSH homeostasis have not been further characterized. That has been the objective of the present studies in which we show that regulation of the basal levels of GCLC and GCLM expression and GSH homeostasis in unstressed cells is the consequence of IKK β signals required to maintain a basal level of NF- κ B activity in the absence of inducers. Inactivation of this pathway markedly reduces cellular GSH and sensitizes cells to cytotoxicity in response to stress stimuli.

MATERIALS AND METHODS

Reagents, antibodies, plasmids and cell culture conditions. The chemical inhibitors of IKK β and NF- κ B and their concentrations of use were 10 μ M JSH, 1 μ M BMS and 0.5 μ M TPCA1, all from Calbiochem-Novabiochem. Antibodies to β -actin were from Pharmingen, to phospho-p65, p65, p50 were from Santa Cruz Biotechnology, Inc. and anti-GCLC and anti-GCLM were a gift from Dr. Ying Chen (University of Cincinnati). Sodium arsenite (As), luminol (5-amino-2,3-dihydro-1,4-phthalazinedione), horseradish peroxidase, catalase and glutathione (GSH) and glutathione disulfide (GSSG) were from Sigma, and TNF α was from Pepro Tech, Inc.

Luciferase reporter plasmids containing binding elements for NF- κ B (NF- κ B-luc) (Tojima et al., 2000), AP-1 (AP1-luc) and NRF2 (Nqo1-luc) (Hoffer et al., 1996) and the *Gclm* (*Gclm*-luc) (Yang et al., 2005b) and *Gclc* (*Gclc*-luc) (Yang et al., 2001b) promoter-driven luciferase plasmids, were described elsewhere. The expression vectors for β -galactosidase were from commercial sources (Fisher Scientific) and for murine GCLC and GCLM were a gift from Dr. Tim Dalton (University of

MOL #61424

Cincinnati). The siGENOME SMARTpool siRNA for mouse *Ikkβ* were from Thermo Scientific (Dharmacon).

All cell culture reagents, including Dulbecco's Modified Eagle's Medium (DMEM), fetal bovine serum (FBS), L-glutamine, MEM nonessential amino acids, penicillin-streptomycin and MEM vitamins were from Invitrogen Corp. The wild type, IKKβ-null, p65-null, TNFR-null and TRAF2-null mouse fibroblasts were described elsewhere (Peng et al., 2007; Lin et al., 2004; Beg et al., 1995) and were maintained in DMEM complete medium with 10% FBS.

Cellular glutathione measurement. The intracellular levels of GSH and GSSG were determined using methods described previously (Senft et al., 2000). Briefly, cells at 90% confluence were washed twice with ice-cold PBS and collected in 300 μl homogenize buffer, containing 154 mM KCl, 5 mM diethylenetriaminepenta-acetic acid (DTPA), 0.1 M KCl and 10 mM MgCl₂ at pH 6.8. After sonication, the homogenates were mixed with 300 μl of RQB-TCA (10% trichloroacetic acid (TCA) in 40mM HCl and 10 mM DTPA). The mixture were subjected to centrifugation at 12,000 g for 10 min at 4 °C. A fraction of the supernatant was reacted with *o*-phthalaldehyde (OPA), which bound to reduced glutathione (GSH) to yield molecules with high quantum yield, and the GSH levels was determined spectrophotofluorometrically as previously described (Senft et al., 2000). Another fraction of the supernatant was treated by dithionite to convert GSSG to GSH and the total GSH+GSSG was determined. Molar GSH and GSSG concentrations were calculated as described by others (Watson and Jones, 2003) and inserted into the Nernst equation,

$$\Delta E' (\text{GSSG} + 2\text{H}^+ \rightarrow 2\text{GSH}) = -240 \text{ mV} - (61.5 \text{ mV}/2e^-) \times \log ([\text{GSH}]^2/[\text{GSSG}])$$

MOL #61424

to estimate redox potentials at pH 7.0.

ROS measurement. Direct detection of intracellular steady-state levels of ROS was carried out on living cells using 2',7'-dichlorofluorescein-diacetate (H₂-DCFDA). Cells cultured on glass coverslips were incubated with 10 μ M CM-H₂-DCFDA (Molecular Probes, Inc., OR) in FBS-free DMEM medium in the dark for 30 min. The cells were washed with PBS and stained with DAPI. ROS generation, resulting in the oxidative production of dichlorofluorescein (excitation, 488 nm; emission, 515–540 nm), was detected using fluorescence microscopy.

Alternatively, cells cultured on 10-cm² plates were trypsinized and resuspended in FBS-free culture medium containing 5 μ M H₂-DCF-DA. After incubation at 37°C for 30 min, cells were washed and suspended in PBS at 1 \times 10⁶ cells/ml. The cells were applied to FACS Calibur analyser (Becton-Dickinson Immunocytometry Systems), which was equipped with a 488 Argon laser for measurements of intracellular fluorescence. Logarithmic detectors were used for the FL-1 fluorescence channel necessary for DCF detection. Mean log fluorescence intensity (MFI) values were obtained by the CELLQUEST software program (Becton-Dickinson).

To measure the concentration of H₂O₂, cells at about 10⁷ cells/ 10-cm² plate were washed twice with KCl-Respiratory Buffer (KRB), consisting of 140 mM KCl, 2.5 mM KH₂PO₄, 2.5 mM MgCl₂, 1.0 mM Na₂-EDTA, 0.05% defatted recrystallized bovine serum albumin, and 5 mM HEPES buffer, pH 7.4. Cells were scraped into KRB at 250 μ g protein/ml. The reaction mixture for H₂O₂ release contained 100 μ g cell protein, 5 mM D(+)-glucose, 5 μ M luminol (5-amino-2,3-dihydro-1,4-phthalazinedione), 2.5 U horseradish peroxidase/ml, in a final volume of 1.0 ml KRB. Catalase (500 U/ml) was added to half the tubes render the assay specific for H₂O₂, since catalase-inhibited luminol

MOL #61424

chemiluminescence is highly specific for H₂O₂ (Shertzer et al., 2004). Chemiluminescence was monitored at 37°C using a Berthold Autolumat Plus luminometer. Luminescence units (LUs) in the presence of catalase were subtracted from LUs in the absence of catalase, and net LU/μg protein plotted against time. Also, the area-under the curves (AUCs) for luminescence versus time were standardized to known H₂O₂ concentrations from 0-50 μM and expressed as nmol H₂O₂/mg protein.

Adenoviral infection. Adenoviruses were used, at a moi of 10 pfu/cell, to infect cells at 60% confluence (Peng et al., 2007). Viral infection was carried out in serum free DMEM for 2 hours with gentle shaking. Following washing with PBS, the cells were maintained in DMEM with 10% FBS for 24 h before being used in experiments.

Cell apoptosis, survival and Western blot analyses. Cell apoptosis was assessed by staining with 4,6-diamidino-2-phenylindole (10 μg/ml DAPI) and fluorescence microscopy observation as described previously (Peng et al., 2007). The cells with condensed or fragmented nuclei were considered to be undergoing apoptosis and the ratio of apoptotic over total cells was thus calculated. Alternatively, apoptosis was evaluated by Annexin V-PE Apoptosis Detection Kit (BD PharmingenTM). Briefly, cells were washed twice with cold PBS and resuspended in 1× Binding Buffer at a concentration of 1×10⁶ cells/ml. 100μl of the solution (1×10⁵ cells) were transferred to a 5 ml culture tube and incubated with 5μl of Annexin V-PE and 5μl of 7-ADD for 15 min at RT in the dark. The cells were analyzed by flow cytometry. The TUNEL assay was performed using ApopTag Plus fluorescein *In Situ* Apoptosis Detection kit according to manufacture's recommendation (CHEMICON). Briefly, the cells cultured on cover slips were first fixed with 1% paraformaldehyde in PBS and post-fixed in precooled ethanol:acetic acid (2:1). The DNA fragments in apoptotic cells were then labeled with the

MOL #61424

digoxigenin-nucleotide, which would bind to the fluorescein conjugated anti-digoxigenin antibody applied subsequently. Finally, the cells were counterstained with DAPI and viewed by fluorescence microscopy. Micrographs of TUNEL positive cells were taken and the percentage of apoptosis was calculated by dividing the number of TUNEL positive cells by the number of total cells in each picture. At least 400 cells for each condition were counted.

Cell viability was determined using the tetrazolium salt MTT (3-(4,5-Dimethylthiazol-2-yl)-2,5-diphenyltetrazolium bromide, a tetrazole), following the manufacturer's specifications (Promega). Western blot analyses were done using whole cell extracts as described previously (Peng et al., 2007).

Cell fractionation. Cytosolic and nuclear extracts were prepared following procedures previously described (Kann et al., 2005). For Western blot analyses, nuclear and cytosolic proteins obtained from 50,000 cells were boiled in SDS-PAGE sample buffer and used for Western blotting analyses using anti-p65.

RNA isolation, Fluorescent labeling of target cDNAs and high-density microarray hybridization and quantitative polymerase chain reaction (QPCR). Total RNA was isolated from *Wild type* and *Ikk β* (-/-) fibroblasts using RNeasy kit (Qiagen) based on the manufacturer's instructions. To verify RNA quality prior to labeling for microarray analyses, samples were analyzed using an Agilent 2100 Bioanalyzer. For microarray work, hybridization probes were from the mouse oligonucleotide library (version 3.0; QIAGEN Operon, Alameda, CA), representing 31,769 annotated mouse genes. Hybridization targets were the paired Cy3- and Cy5-labeled control and test cDNAs synthesized from 20 μ g of total RNA by an oligo(dT)-primed, reverse transcriptase reaction and were labeled with

MOL #61424

monofunctional reactive Cy3 and Cy5 (Amersham, Piscataway, NJ). After hybridization under high-stringency conditions, slides were washed and simultaneously scanned at a 10- μ m resolution at 635 (Cy5) and 532 (Cy3) nm (GenePix 4000B; Axon Instruments, Inc., Union City, CA). Comparisons were carried out with triplicate biological replicates using flipped dye arrays to allow for the removal of gene-specific dye effects. Data normalization was performed in three steps for each microarray.

For quantitative real-time PCR analyses, cDNA was synthesized by reverse transcription of 1 - 20 μ g total RNA using SuperScript™ II RNase H⁻ reverse transcriptase (Invitrogen). The cDNA was subjected to quantitative PCR using an MX3000p thermal cycler system and SYBR Green QPCR Master Mix (Stratagene). The conditions for the PCR amplification were optimized for specific PCR reactions. At the end of the PCR the samples were subjected to melting curve analysis. All reactions were performed at least in triplicate. Oligonucleotides used as the specific primers to amplify mouse genes cDNA are as following: *Gclc*, 5' ATGACTGTTGCCAGGTGGATGAGA and 5' ACACGCCATCCTAACAGCGATCA; *Gclm*, 5' AGCTGGACTCTGTGATCATGGCTT and 5' CAAAGGCAGTCAAATCTGGTGGCA; *Gapdh*, 5' CCATGGAGAAGGCTGGGG and 5' CAAAGTTGTCATGGATGACC; *Ikk β* , 5' CTCGAACTGGTTCAAGTATCTTCGG and 5' AACAGATCGCCATCAAGCAATGCC

Transfection and luciferase reporter assay. The *Ikk β* (-/-) cells were grown to 60%-70% confluence on 10-cm² plate. The cells were transiently transfected with 10 μ g of either vector control, or expression vectors for *Gclc* and/or *Gclm* together with 2 μ g puromycin expression vector. At 12 h post-transfection, the cells were grown in selection medium containing 1 μ g/ml puromycin for 48 h and were used for experiments.

MOL #61424

Transfection of *Ikkβ*-siRNA was performed using HiperFect transfection reagent (QIAGEN) with fast-forward transfection protocol according to manufacture's recommendation. Briefly, on the day of transfection, 5×10^6 WT MEF cells were seeded in a 10-cm² plate containing 6 ml of regular culture medium, followed by adding 2 ml DMEM mixed with 0.8 nmol siRNA (this would give a final siRNA concentration of 100 nM) and 200 μ l transfection reagent into the plate. The cells were incubated under normal culture condition for 48 h before further experiment.

Cells seeded in 24-well tissue culture plates at 1×10^5 cells/well were grown for 16 h before transfection. Transfection was carried out using Lipofectamine Plus reagent (Invitrogen), 0.5 μ g luciferase reporter and 0.1 μ g β -galactosidase plasmids/well, following the manufacturer's instructions. Twenty-four hours after transfection, cells were deprived of serum overnight and subjected to the indicated treatments for 16 hours. Cells were lysed and luciferase activity and β -galactosidase activity were determined using the luciferase reporter and β -galactosidase reporter kits (Promega).

Chromatin Immunoprecipitation (ChIP) Analyses. ChIP was performed using wild type and *Ikkβ* (-/-) cells using methods described (Schnekenburger et al., 2007). Briefly, cells were treated with formaldehyde and chromatin was prepared and sheared to a size range of 0.3–0.6 kb by sonication in a crushed-ice/water bath with six 30-s bursts of 200 W, with a 30-s interval between bursts using a Bioruptor (Diagenode). Chromatin was immunoprecipitated overnight using antibodies for c-JUN, NF κ B p50/p65 and nonspecific rabbit IgG. The immune complexes were allowed to react with protein A-agarose beads (Millipore) and after extensive washing, the precipitates were removed from the beads using elution buffer (50 mM NaHCO₃ and 1% SDS) and mild vortexing. The cross-linking was reversed and the samples were sequentially digested with RNase A and proteinase K. Precipitated DNA was purified by chromatography on QIAquick columns (QIAGEN) and subjected to real-time PCR. For a

MOL #61424

complete coverage of the region between – 2.0 kbp and + 1 bp of the mouse *Gclc* and – 1.5 kbp and + 0.5 kbp of the mouse *Gclm* promoters, 5 primer sets were designed for each gene and tested in PCR reactions with genomic DNA as the template. For the purpose of size confirmation, end-point PCR products were separated by electrophoresis through 15% polyacrylamide gels and visualized after staining with ethidium bromide. Relative cycle differences in QRT-PCR were determined using ΔC_T determined by the cycle threshold (C_T) value of ChIP DNA normalized to the C_T of input DNA. QPCR results are shown as fold-changes of specific antibody immunoprecipitation over IgG non-specific immunoprecipitation controls.

Statistical analysis. Statistical analyses of microarray data were performed by fitting the mixed-effects linear model for each gene separately, as discussed in detail previously (Kann et al., 2005). Resulting t statistics from each comparison were then adjusted using a hierarchical empirical Bayes model (Smyth, 2004) for calculation of P values and using the expected number of false positives based on the false discovery rate (Klipper-Aurbach et al., 1995). For other statistical analyses, comparisons were performed using Student's two-tailed paired t -test or multiple comparison ANOVA.

RESULTS

Genetic and pharmacological inactivation of the canonical IKK β pathway causes GSH deficiency.

Previously, we have shown that fibroblasts deficient in IKK β have high level of ROS accumulation in response to arsenic and are extremely sensitive to arsenic toxicity (Peng et al., 2007). In this regard, *Ikk β* (-/-) cells are similar to cells deficient in glutathione, which also have a high prooxidant status (Kann et al., 2005). To test whether the susceptibility of IKK β -null cells to oxidative stress induced by arsenic was also related to glutathione deficiency, we measured intracellular GSH and GSSG levels

MOL #61424

and calculated the corresponding redox couple potentials. Reduced GSH levels were high at 31 nmole/mg protein in wild type cells and were nearly 5-times lower in *Ikkβ*^(-/-) cells (Fig. 1A). The redox potential of the GSSG/2GSH couple was calculated (Watson and Jones, 2003) to be -176 mV in wild type cells and was decreased to half that level in *Ikkβ*^(-/-) cells. Expression of IKKβ, but not β-galactosidase, in the *Ikkβ*^(-/-) cells significantly elevated GSH contents and reducing potential of the redox couple (Fig. 1A), indicating that the effects seen in the *Ikkβ*^(-/-) were primarily due to the lack of IKKβ and not to compensatory mechanisms established during embryonic development.

In the classical NF-κB pathway, IKKβ is responsible for transmitting signals from upstream TNFR1 and TRAF2/5 to downstream p65/RelA. To test whether other components of this pathway were also involved in modulating redox potential, we measured GSH and GSSG values in cells deficient in TNFR1, TRAF2 and p65 (Fig. 1A). Both TNFR1 and p65 are essential for pathway activation and correspondingly, the *Tnfr1*^(-/-) and *p65*^(-/-) cells had nearly 80% reduction of GSH in comparison to the wild type cells. TRAF2, on the other hand, is dispensable for classical pathway activation and the *Traf2*^(-/-) had only 50% GSH reduction. Similarly, the reducing potential was decreased significantly in *Tnfr1*^(-/-) and *p65*^(-/-) cells and less so in *Traf2*^(-/-) cells. Based on these studies, we suggest that the classical IKK pathway is required for maintaining the homeostatic levels of GSH in mouse fibroblasts.

While the physiologic role of the IKKβ pathway has been mostly studied using genetic inactivation of IKKβ in mice, *IKKβ* gene mutations have not been found in homozygosity linked to human diseases. In clinical settings, pharmaceutical inhibition of IKKβ signaling is commonly used for anti-inflammation and pain alleviation purposes, posing the question of whether IKKβ or NF-κB

MOL #61424

inhibition by chemicals may achieve effects similar to those of genetic IKK β ablation. We chose three commercially available inhibitors, JSH23, a cell-permeable diamino compound that blocks p65/RelA nuclear translocation and activation, BMS-345541 and TPCA-1, potent and specific inhibitors of IKK β , to evaluate the consequence of IKK β and NF- κ B inhibition. Treatment of wild type fibroblasts with these inhibitors caused reduced GSH content and lower redox potential (Fig. 1B). Thus, genetic and pharmaceutical inactivation of the NF- κ B pathway are similar, in the sense that they both cause inhibition of basal NF- κ B activity, reduction of GCL expression, and decrease of intracellular GSH and redox potential.

Loss of IKK β signaling sensitizes cells to the cytotoxicity of pharmacological and environmental agents.

GSH is one of the most important anti-oxidants that protect the organism against a broad range of physiological and environmental stresses (Meister and Anderson, 1983; Townsend et al., 2003). We asked whether IKK β -deficient cells, with reduced GSH levels, were more vulnerable to stress toxicity. We treated wild type and IKK β -deficient cells with various stress stimuli and evaluated cell survival. The treatments include the oxidative stress inducer H₂O₂, the DNA damaging agents etoposide and cisplatin, and the microtubule toxins taxol and colchicine, (Kurosu et al., 2003; Alexandre et al., 2006; Varbiro et al., 2001; Taniguchi et al., 2005). Relative to wild type cells, *Tnfr1*(-/-) and *Ikk β* (-/-) cells and to a lesser extent *Traf2*(-/-) cells, showed decreased survival in response to all five stress stimuli (Fig. 2A). Arsenic is an environmental toxic agent that can modify mitochondrial respiration, leading to ROS production and cell apoptosis (Ralph, 2008). We found that genetic knockout (Fig. 2A) and knockout down (Figs. 2B and 2C) of *Ikk β* and pharmacological inactivation (Fig. 2D) of IKK β signaling significantly enhanced arsenic toxicity. These findings

MOL #61424

strongly suggest that IKK β signaling is required for protecting cells against oxidative stress elicited by pharmacological and environmental agents.

Reduced GCLC and GCLM expression in *Ikk β* (-/-) cells. Using DCF-DA, we detected a slightly elevated ROS in the *Tnfr1*(-/-), *Traf2*(-/-) and *Ikk β* (-/-) cells compared to the wild type cells (Fig. 3A). Similarly, using luminol chemiluminescence, we found the H₂O₂ levels were slightly elevated in *Traf2*(-/-), but significantly increased in *Tnfr1*(-/-) and *Ikk β* (-/-), compared to wild type cells (Fig. 3B). The higher ROS in the knockout cells, however, was insufficient to cause a significant change in GSH oxidation, because the levels of GSSG were the same in wild type and IKK β -deficient cells (Fig. 1A). Thus, we suggest that GSH deficiency in the IKK β deficient cells was not due to increased oxidative GSH depletion.

Alternatively, GSH deficiency in IKK β -deficient cells could be due to increase in GSH exportation. To determine whether this was the case, we measured extracellular GSH content in the growth media. The extracellular GSH was low overall, but it corresponded well with the intracellular levels in the different cells tested. Thus, the wild type and Ad-IKK β infected *Ikk β* (-/-) cells had slightly higher levels of extracellular GSH than the IKK β -deficient cells (Fig. S1). GSH exportation to the extracellular milieu is mediated by ATP-binding cassette transporters (ABCCs). In a genome-wide expression profiling experiment, we found no apparent differences in the levels of *Abcc1*, 2, 3, 4, 5, 6, 8, 9, 10 12 mRNA in wild type and *Ikk β* (-/-) cells (data not shown). Together, these observations suggest that IKK β signaling helps to maintain cellular GSH through mechanisms independent of GSH consumption or export.

MOL #61424

Glutathione homeostasis depends critically on a set of glutathione redox cycling enzymes. GCL and GS are responsible for biosynthesis and GSR for reduction of GSSG to GSH. On the other hand, GPX and CYP2E1 catalyze GSH to generate oxidized GSSG. In genome-wide expression studies, we found that IKK β ablation caused a significant reduction in *Gclc* and *Gclm* mRNA, while it had less effect on the levels of other GSH redox cycling enzymes (Table I). Using real-time RT-PCR, we further confirmed that the *Ikk β* (-/-) cells had 58% reduction of *Gclc* and 67% reduction of *Gclm* mRNA in comparison to wild type cells (Fig. 3C). Correspondingly, the *Ikk β* (-/-) cells had reduced GCLC and GCLM proteins. Reconstitution of IKK β expression in the *Ikk β* (-/-) cells markedly elevated the GCLC and GCLM proteins (Fig. 3D), while on the other hand, treatment of wild type cells with IKK β signaling inhibitors markedly reduced the levels of both *Gclc* and *Gclm* (Fig. 3E). These observations support a role for IKK β signaling in optimal GCLC and GCLM expression.

IKK β -dependent NF- κ B binding and activation of the *Gcl* promoters. To address whether the IKK β pathway was required for transcriptional activation of the *Gclc* and *Gclm* promoters, we measured *Gclc*- and *Gclm*-promoter driven luciferase activities in wild type and knockout cells (Fig. 4A). Compared to wild type cells, *Gclc*-luciferase activity was decreased slightly in *Traf2* (-/-), but reduced markedly in *Ikk β* (-/-) and more so in *Tnfr1* (-/-) cells. Similarly, *Gclm*-luciferase activity was reduced by 60-80% in *Tnfr1* (-/-), *Ikk β* (-/-) and *Traf2* (-/-) cells compared to wild type cells.

The transcription factors NF- κ B, AP-1 and NRF2 mediate *Gclc* and *Gclm* gene induction (Yang et al., 2005b; Yang et al., 2005a). To identify which of these factors might act downstream of the IKK β signaling in the regulation of the *Gcl* promoters, we measured the activity of each transcription factor in wild type and knockout cells using luciferase reporter systems. We found the basal NF- κ B activity

MOL #61424

was highest in wild type and IKK β -reconstituted *Ikk β* (-/-) cells, slightly lower in *Traf2* (-/-) cells, but much reduced in *Ikk β* (-/-) and *Tnfr1* (-/-) cells (Fig. 4B). Examination of nuclear localization of active RelA/p65 led to the same conclusion. Approximately 10 % of the total RelA/p65 was found in the nucleus of wild type cells and 1 % in the nucleus of *Traf2*(-/-) cells, while there was no detectable nuclear RelA/p65 in *Ikk β* (-/-) or *Tnfr1* (-/-) cells (Fig. 4C). TNF α further potentiated NF- κ B activity and nuclear translocation in wild type and *Traf2* (-/-), but it caused very little, if any, NF- κ B activation in *Tnfr1* (-/-) and *Ikk β* (-/-) cells (Figs. 4C and S2). Treatment of the wild type cells with IKK β signaling inhibitors prevented basal and TNF α induced p65/RelA nuclear translocation and reduced significantly NF- κ B activity, similar to the effects of genetic IKK β pathway inactivation (Figs. 4C and 4D). Importantly, there was a good correlation between basal activities of NF- κ B and *Gcl* promoters in all the experimental conditions examined. In contrast, we found that the basal NRF2 and AP-1 activities were not reduced, but were rather increased in *Ikk β* (-/-) and *p65*(-/-) cells relative to wild type or IKK β -reconstituted *Ikk β* (-/-) cells, making it unlikely that these factors were involved in IKK β -dependent *Gcl* promoter activation (Fig. 4E).

Potential binding sites for NF- κ B were found using CHIPMAPPER (www.ChipMapper.com) throughout the 2-kb regions in the mouse *Gclc* and *Gclm* promoters. To assess whether NF- κ B directly interacts with the *Gclc* and *Gclm* promoters, we performed chromatin-immunoprecipitation (ChIP) assays (Fig. 5). The ChIP results showed that p65/p50 NF- κ B interacts with regions in both distal and proximal *Gclc* and *Gclm* promoters with higher efficiency in wild type than in *Ikk β* (-/-) cells. In contrast, c-JUN interacts with a distal region of the *Gclc* promoter with higher efficiency in *Ikk β* (-/-) cells, consistent with higher c-JUN activities in these cells. In the unstressed fibroblasts, we did not

MOL #61424

detect direct c-JUN interactions with the mouse *Gclm* promoter. These observations argue against a positive regulatory role of c-JUN in *Gclc* and *Gclm* promoter activation in unstressed conditions, but on the other hand, suggest that a more abundant NF- κ B occupancy of the *Gclc* and *Gclm* promoters may be responsible for higher promoter activation in wild type cells.

Increased GCLC and GCLM expression elevates GSH in *Ikk β* (-/-) cells. To test whether the reduced GCLC and GCLM expression was responsible for GSH deficiency in the *Ikk β* (-/-) cells, we introduced transiently either empty, GCLC or GCLM expression vectors into *Ikk β* (-/-) cells and measured GSH and GSSG. The GSH levels were significantly elevated in GCLC- and GCLM-overexpressing *Ikk β* (-/-) cells with levels 2- to 3-fold higher than those in cells transfected with the empty vector (Fig. 6A). Correspondingly, the reducing potential in the *Ikk β* (-/-) cells was increased from $\Delta E'$ -49 mV to -165 mV with GCLC ectopic expression and to -127 mV with GCLM ectopic expression.

Exogenous GCLC and GCLM expression in the *Ikk β* (-/-) cells also effectively prevented the induction of ROS by arsenic, as DCFDA positive *Ikk β* (-/-) cells were easily detectable in control, vector-transfected cells, but not in *Gclc/Gclm* transfected cells (Fig. 6B). Concurrently, the *Gclc/Gclm* transfected *Ikk β* (-/-) cells were protected from arsenic-induced apoptosis (Fig. 6C and 6D). Hence, IKK β -mediated optimal GCLC and GCLM expression helps to maintain cellular GSH levels and electronegative $\Delta E'$ values, which in turn is required for protecting cells against oxidative stress toxicity.

DISCUSSION

MOL #61424

The classical IKK β -NF- κ B pathway has a fundamental role in modulating innate and adaptive immune responses. In this context, activation of this pathway leads to immediate induction of pro-inflammatory cytokines, such as TNF α , that, in addition to their anti-pathogenic effect, can further activate the IKK β -NF- κ B pathway, thereby propagating and amplifying the inflammatory responses. Recent genetic and chemical inhibitor studies have uncovered new functions of this pathway that may not be directly linked to inflammation (Hayden and Ghosh, 2008). Here we show that basal low level activation of the IKK β -NF- κ B pathway plays a pivotal role in maintaining GSH homeostasis. Genetic and pharmacological inactivation of this pathway results in severe glutathione deficiency that leads to increased sensitivity to toxicity caused by a broad range of environmental and therapeutic agents.

Both basal and TNF α -induced NF- κ B activities are greatly reduced in *Traf2* (-/-) and almost completely abolished in *Tnfr1* (-/-) and *Ikk β* (-/-) cells. This observation supports the idea that the TNF α -induced classical IKK β cascade is normally maintained at a low constitutively active state, leading to slow I κ B α degradation and steady state NF- κ B activation, while excessive exogenous TNF α accelerates and amplifies this reaction, causing more abundant NF- κ B activation (O'Dea et al., 2008). While robust activation of the IKK β -NF- κ B pathway is known to activate pro-inflammatory transcriptional programs, the basal NF- κ B activity may dictate different transcription trajectories. We show that IKK β ablation affects the expression of genes involved in GSH homeostasis, important for maintenance of biological systems (Chen et al., 2003; Peng et al., 2007). Because NF- κ B is known to be activated by low levels of ROS and inhibited by anti-oxidants (Mantena and Katiyar, 2006), maintaining GSH homeostasis may serve as an autocrine regulatory mechanism through which the IKK β -NF- κ B pathway feedbacks to keep its own activity in check.

MOL #61424

The NF- κ B is required for optimal expression of anti-oxidants, including the cytochrome p450 CYP1B1, MnSOD, FHL and metallothionein (Pham et al., 2004;Chen et al., 2003;Peng et al., 2007;Kamata et al., 2005); however, none of these known NF- κ B targets has a major role in GSH homeostasis. We find that the IKK β -dependent NF- κ B transcription factor directly interacts with the *Gclc* and *Gclm* promoters and that the extent of the binding correlates with the level of GCLC/GCLM expression and GSH content. Induction of the *Gclc* and *Gclm* promoters under oxidative stress conditions is mediated by redox sensitive transcription factors (Yang et al., 2001b;Yang et al., 2001a;Jeyapaul and Jaiswal, 2000;Nagashima et al., 2007;Lu, 2008). Specifically, stress-activated NRF2 up-regulates AP-1 and NF- κ B, which in turn bind to and activate the *Gclc* and *Gclm* promoters (Urata et al., 1996;Yang et al., 2005b;Yang et al., 2005a). We find that the IKK β -null cells have slightly higher AP-1 and NRF2 activities probably due to elevated ROS (Fig. 3A), but they have lower NF- κ B activity, corresponding to lower *Gcl* promoter activation. Thus, maintenance of basal *Gcl* promoter activity under normal non-stress condition appears to depend on IKK β -mediated NF- κ B, not on c-JUN- or NRF2-mediated NF- κ B induction. These observations further suggest that the transcriptional machinery involved in maintaining the basal activity of the *Gcl* promoters is different from that activated by physiological and environmental stresses.

GSH is an abundant thiol-containing small molecule that plays an evolutionarily conserved role in maintaining an intracellular reducing environment (Meister and Anderson, 1983). Low levels of GCLC/GCLM expression in cells deficient in IKK β may lead to GSH deficiency and ultimately may be responsible for a wide variety of diseases resulting from excess oxidative stress, including cancer, neurodegenerative disorders and aging (Townsend et al., 2003). In this regard, GSH deficiency

MOL #61424

resulting from inactivation of the IKK β -NF- κ B pathway may be responsible for some of the physiological and pathological phenomena observed in *Ikk β* (-/-) mice, such as those occurring in chemically induced liver carcinogenesis and increased insulin sensitivity. Hence, pharmacological inhibition of the IKK β -NF- κ B pathway may not only suppress inflammatory responses, but also cause GSH deficiency, leading to broader and long-term physio-pathological consequences.

ACKNOWLEDGEMENTS

We thank Drs. Michael Karin for *Ikk β* (-/-) MEFs, Ebrahim Zandi for *Ikk β* (-/-)-R cells, Sankar Ghosh for *p65*(-/-), Yinling Hu for IKK β adenovirus, Tim Dalton, Daniel Nebert and Ying Chen for the *Gclc/Gclm* expression vectors and the GCLC/M antibodies and Dr. Shelly C. Lu for *Gclc-Luc/Gclm-Luc* plasmids.

MOL #61424

REFERENCES

- Alexandre J, Batteux F, Nicco C, Chereau C, Laurent A, Guillevin L, Weill B and Goldwasser F (2006) Accumulation of Hydrogen Peroxide Is an Early and Crucial Step for Paclitaxel-Induced Cancer Cell Death Both in Vitro and in Vivo. *Int J Cancer* **119**:41-48.
- Beg AA, Sha W C, Bronson R T, Ghosh S and Baltimore D (1995) Embryonic Lethality and Liver Degeneration in Mice Lacking the RelA Component of NF-Kappa B. *Nature* **376**:167-170.
- Boitier E, Merad-Boudia M, Guguen-Guillouzo C, Defer N, Ceballos-Picot I, Leroux J P and Marsac C (1995) Impairment of the Mitochondrial Respiratory Chain Activity in Diethylnitrosamine-Induced Rat Hepatomas: Possible Involvement of Oxygen Free Radicals. *Cancer Res* **55**:3028-3035.
- Chen F, Castranova V, Li Z, Karin M and Shi X (2003) Inhibitor of Nuclear Factor KappaB Kinase Deficiency Enhances Oxidative Stress and Prolongs C-Jun NH2-Terminal Kinase Activation Induced by Arsenic. *Cancer Res* **63**:7689-7693.
- Cosulich SC, James N H, Needham M R, Newham P P, Bundell K R and Roberts R A (2000) A Dominant Negative Form of IKK2 Prevents Suppression of Apoptosis by the Peroxisome Proliferator Nafenopin. *Carcinogenesis* **21**:1757-1760.
- Hayden MS and Ghosh S (2008) Shared Principles in NF-KappaB Signaling. *Cell* **132**:344-362.
- Hoffer A, Chang C Y and Puga A (1996) Dioxin Induces Transcription of Fos and Jun Genes by Ah Receptor-Dependent and -Independent Pathways. *Toxicol Appl Pharmacol* **141**:238-47.
- Jeyapaul J and Jaiswal A K (2000) Nrf2 and C-Jun Regulation of Antioxidant Response Element (ARE)-Mediated Expression and Induction of Gamma-Glutamylcysteine Synthetase Heavy Subunit Gene. *Biochem Pharmacol* **59**:1433-1439.
- Kamata H, Honda S, Maeda S, Chang L, Hirata H and Karin M (2005) Reactive Oxygen Species Promote TNFalpha-Induced Death and Sustained JNK Activation by Inhibiting MAP Kinase Phosphatases. *Cell* **120**:649-661.
- Kann S, Estes C, Reichard J F, Huang M Y, Sartor M A, Schwemberger S, Chen Y, Dalton T P, Shertzer H G, Xia Y and Puga A (2005) Butylhydroquinone Protects Cells Genetically Deficient in Glutathione Biosynthesis From Arsenite-Induced Apoptosis Without Significantly Changing Their Prooxidant Status. *Toxicol Sci* **87**:365-384.
- Klipper-Aurbach Y, Wasserman M, Braunspiegel-Weintrob N, Borstein D, Peleg S, Assa S, Karp M, Benjamini Y, Hochberg Y and Laron Z (1995) Mathematical Formulae for the Prediction of the

MOL #61424

Residual Beta Cell Function During the First Two Years of Disease in Children and Adolescents With Insulin-Dependent Diabetes Mellitus. *Med Hypotheses* **45**:486-490.

Kurosu T, Fukuda T, Miki T and Miura O (2003) BCL6 Overexpression Prevents Increase in Reactive Oxygen Species and Inhibits Apoptosis Induced by Chemotherapeutic Reagents in B-Cell Lymphoma Cells. *Oncogene* **22**:4459-4468.

Lin Y, Choksi S, Shen H M, Yang Q F, Hur G M, Kim Y S, Tran J H, Nedospasov S A and Liu Z G (2004) Tumor Necrosis Factor-Induced Nonapoptotic Cell Death Requires Receptor-Interacting Protein-Mediated Cellular Reactive Oxygen Species Accumulation. *J Biol Chem* **279**:10822-10828.

Lu SC (2008) Regulation of Glutathione Synthesis. *Mol Aspects Med*.

Maeda S, Kamata H, Luo J L, Leffert H and Karin M (2005) IKKbeta Couples Hepatocyte Death to Cytokine-Driven Compensatory Proliferation That Promotes Chemical Hepatocarcinogenesis. *Cell* **121**:977-990.

Mantena SK and Katiyar S K (2006) Grape Seed Proanthocyanidins Inhibit UV-Radiation-Induced Oxidative Stress and Activation of MAPK and NF-KappaB Signaling in Human Epidermal Keratinocytes. *Free Radic Biol Med* **40**:1603-1614.

Meister A and Anderson M E (1983) Glutathione. *Annu Rev Biochem* **52**:711-760.

Nagashima R, Sugiyama C, Yoneyama M, Kuramoto N, Kawada K and Ogita K (2007) Acoustic Overstimulation Facilitates the Expression of Glutamate-Cysteine Ligase Catalytic Subunit Probably Through Enhanced DNA Binding of Activator Protein-1 and/or NF-KappaB in the Murine Cochlea. *Neurochem Int* **51**:209-215.

O'Dea EL, Kearns J D and Hoffmann A (2008) UV As an Amplifier Rather Than Inducer of NF-KappaB Activity. *Mol Cell* **30**:632-641.

Pahl HL (1999) Activators and Target Genes of Rel/NF-KappaB Transcription Factors. *Oncogene* **18**:6853-6866.

Peng Z, Peng L, Fan Y, Zandi E, Shertzer H G and Xia Y (2007) A Critical Role for IkappaB Kinase Beta in Metallothionein-1 Expression and Protection Against Arsenic Toxicity. *J Biol Chem* **282**:21487-21496.

Pham CG, Bubici C, Zazzeroni F, Papa S, Jones J, Alvarez K, Jayawardena S, De S E, Cong R, Beaumont C, Torti F M, Torti S V and Franzoso G (2004) Ferritin Heavy Chain Upregulation by NF-

MOL #61424

KappaB Inhibits TNFalpha-Induced Apoptosis by Suppressing Reactive Oxygen Species. *Cell* **119**:529-542.

Ralph SJ (2008) Arsenic-Based Antineoplastic Drugs and Their Mechanisms of Action 1. *Met Based Drugs* **2008**:260146.

Sakon S, Xue X, Takekawa M, Sasazuki T, Okazaki T, Kojima Y, Piao J H, Yagita H, Okumura K, Doi T and Nakano H (2003) NF-KappaB Inhibits TNF-Induced Accumulation of ROS That Mediate Prolonged MAPK Activation and Necrotic Cell Death. *EMBO J* **22**:3898-3909.

Schnekenburger M, Talaska G and Puga A (2007) Chromium Cross-Links Histone Deacetylase 1-DNA Methyltransferase 1 Complexes to Chromatin, Inhibiting Histone-Remodeling Marks Critical for Transcriptional Activation. *Mol Cell Biol* **27**:7089-7101.

Senft AP, Dalton T P and Shertzer H G (2000) Determining Glutathione and Glutathione Disulfide Using the Fluorescence Probe O-Phthalaldehyde. *Anal Biochem* **280**:80-86.

Shertzer HG, Clay C D, Genter M B, Chames M C, Schneider S N, Oakley G G, Nebert D W and Dalton T P (2004) Uncoupling-Mediated Generation of Reactive Oxygen by Halogenated Aromatic Hydrocarbons in Mouse Liver Microsomes. *Free Radic Biol Med* **36**:618-631.

Sierra-Rivera E, Meredith M J, Summar M L, Smith M D, Voorhees G J, Stoffel C M and Freeman M L (1994) Genes Regulating Glutathione Concentrations in X-Ray-Transformed Rat Embryo Fibroblasts: Changes in Gamma-Glutamylcysteine Synthetase and Gamma-Glutamyltranspeptidase Expression. *Carcinogenesis* **15**:1301-1307.

Smyth GK (2004) Linear Models and Empirical Bayes Methods for Assessing Differential Expression in Microarray Experiments. *Stat Appl Genet Mol Biol* **3**:Article3.

Taniguchi T, Takahashi M, Shinohara F, Sato T, Echigo S and Rikiishi H (2005) Involvement of NF-KappaB and Mitochondrial Pathways in Docetaxel-Induced Apoptosis of Human Oral Squamous Cell Carcinoma. *Int J Mol Med* **15**:667-673.

Tojima Y, Fujimoto A, Delhase M, Chen Y, Hatakeyama S, Nakayama K, Kaneko Y, Nimura Y, Motoyama N, Ikeda K, Karin M and Nakanishi M (2000) NAK Is an IkappaB Kinase-Activating Kinase. *Nature* **404**:778-782.

Townsend DM, Tew K D and Tapiero H (2003) The Importance of Glutathione in Human Disease. *Biomed Pharmacother* **57**:145-155.

MOL #61424

Urata Y, Yamamoto H, Goto S, Tsushima H, Akazawa S, Yamashita S, Nagataki S and Kondo T (1996) Long Exposure to High Glucose Concentration Impairs the Responsive Expression of Gamma-Glutamylcysteine Synthetase by Interleukin-1beta and Tumor Necrosis Factor-Alpha in Mouse Endothelial Cells. *J Biol Chem* **271**:15146-15152.

Varbiro G, Veres B, Gallyas F, Jr. and Sumegi B (2001) Direct Effect of Taxol on Free Radical Formation and Mitochondrial Permeability Transition. *Free Radic Biol Med* **31**:548-558.

Watson WH and Jones D P (2003) Oxidation of Nuclear Thioredoxin During Oxidative Stress. *FEBS Lett* **543**:144-147.

Yang H, Magilnick N, Lee C, Kalmaz D, Ou X, Chan J Y and Lu S C (2005a) Nrf1 and Nrf2 Regulate Rat Glutamate-Cysteine Ligase Catalytic Subunit Transcription Indirectly Via NF-KappaB and AP-1. *Mol Cell Biol* **25**:5933-5946.

Yang H, Magilnick N, Ou X and Lu S C (2005b) Tumour Necrosis Factor Alpha Induces Co-Ordinated Activation of Rat GSH Synthetic Enzymes Via Nuclear Factor KappaB and Activator Protein-1. *Biochem J* **391**:399-408.

Yang H, Wang J, Huang Z Z, Ou X and Lu S C (2001a) Cloning and Characterization of the 5'-Flanking Region of the Rat Glutamate-Cysteine Ligase Catalytic Subunit. *Biochem J* **357**:447-455.

Yang H, Wang J, Ou X, Huang Z Z and Lu S C (2001b) Cloning and Analysis of the Rat Glutamate-Cysteine Ligase Modifier Subunit Promoter. *Biochem Biophys Res Commun* **285**:476-482.

MOL #61424

Footnotes

This work is supported in part by Public Health Service grants from the National Institute of Environmental Health Sciences ES 11798, ES10708, ES06096 and Environmental Carcinogenesis and Mutagenesis (T32ES007250) training program and from the National Eye Institute EY15227.

MOL #61424

LEGENDS FOR FIGURES

Figure 1. Genetic and pharmacological IKK β pathway inactivation causes GSH deficiency. (A)

Wild type, knockout and *Ikk β* (-/-) cells infected with Ad β -gal [β (-/-)- β -gal] or Ad IKK β [β (-/-)-IKK β], and (B) Wild type fibroblasts treated for 24 h with 0.1% DMSO, 10 μ M JSH, 1 μ M BMS and 0.5 μ M TPCA1, as indicated, were collected and cell lysates were used for measurement of GSH and GSSG contents and calculation of GSH/GSSH redox potentials. All results are presented as the mean values \pm S.E. from at least three independent experiments. Statistical analyses were done in comparison to the mean values in control wild type cells and ** $p < 0.01$, *** $p < 0.001$ were considered significant.

Figure 2. IKK β and NF- κ B inactivation reduces cell survival in response to oxidative damage.

(A) Wild type and gene-knockout fibroblasts were treated for 24 h with various oxidative agents, including 10 μ M sodium arsenite (As), 50 μ M hydrogen peroxide (H₂O₂), 50 μ M cisplatin (Cispl), 50 μ M etoposide (Etop), 5 μ M taxol and 5 μ M nocodazole (Nocod). Cell viability was measured by MTT assay. (B) Wild type fibroblasts were transfected with either scrambled or *Ikk β* -siRNA (100 nM). The relative *Ikk β* expression was determined by real-time RT-PCR. The *Ikk β* levels in scrambled RNA transfected cells are designated as 1. (C) The wild type cells with or without *Ikk β* -siRNA transfection and *Ikk β* (-/-) cells were treated with 50 μ M arsenic for 2 h. Apoptosis was measured by TUNEL assay. The values represent the average of at least 400 cells counted. (D) Wild type fibroblasts treated for 2 h with 0.1% DMSO, 10 μ M JSH, 1 μ M BMS and 0.5 μ M TPCA1, followed by treatment with 10 μ M sodium arsenite for 24 h. Cell viability was measured by MTT assay. All results are presented as the mean values \pm S.E. from at least three independent experiments. Statistical analyses

MOL #61424

were done in comparison to the mean values in control wild type cells and ** $p < 0.01$, *** $p < 0.001$ were considered significant.

Figure 3. Inactivation of the IKK β pathway reduces GCLC and GCLM expression. Wild type, *Ikk β* (-/-), *Tnfr1*(-/-) and *Traf2*(-/-) cells were (A) labeled with CM-H2DCFDA under normal growth conditions and were analyzed by Flow cytometry, and (B) used for measurement of H₂O₂ release by catalase-inhibited luminol chemiluminescence. The time-courses for H₂O₂ release are shown in the line plots as luminescence units (LU)/ μ g cell protein, with the insert depicting the area under each curve (AUC) as nmol H₂O₂ release/mg protein. Each value represents the average of 2 experiments. Total RNA isolated from (C) wild type and *Ikk β* (-/-) cells, and (E) wild type cells treated for 24 h with 0.1% DMSO, 10 μ M JSH, 1 μ M BMS and 0.5 μ M TPCA1. The RNA were subjected to reverse transcription followed by q-RT-PCR. Results showed the levels of *Gclc/Gapdh* and *Gclm/Gapdh* in *Ikk β* (-/-) relative to those in wild type cells designated as 1. (D) Total cell lysates from wild type, *Ikk β* (-/-) and *Ikk β* (-/-)-infected with IKK β adenovirus were subjected to Western blotting. The GCLC/ β -actin and GCLM/ β -actin levels were compared to the levels in wild type cells designated as 1. All results are presented as the mean values \pm S.E. from at least three independent experiments. Statistical analyses were done in comparison to the mean values in control wild type cells and ** $p < 0.01$, *** $p < 0.001$ were considered significant.

Figure 4. Inactivation of the IKK β pathway affects transcription factor activities. (A) Wild type, *Ikk β* (-/-), *Tnfr1*(-/-) and *Traf2*(-/-) cells were transfected with β -gal expression plasmids together with *Gclc*-Luc and *Gclm*-Luc. The relative luciferase activities were normalized to β -galactosidase activities measured 24 hours after transfection. Wild type, various knockout cells and *Ikk β* (-/-) cells

MOL #61424

infected with Ad IKK β [β (-/-)-IKK β] were transiently transfected with β -gal expression plasmids, together with (B) and (E) AP-1-luc and Nqo1-luc, respectively. (D) Wild type cells were transfected with NF- κ B-luc and β -gal plasmids for 24 h, followed by inhibitor and TNF α treatment for 16 h. The relative luciferase activities were normalized to β -galactosidase activities measured 24 hours after transfection. All results are presented as the mean values \pm S.E. from at least three independent experiments. Statistical analyses were done in comparison to the mean values in control wild type cells and ** $p < 0.01$, *** $p < 0.001$ were considered significant. (C) Cells were either untreated or treated with TNF α (10 ng/ml) for 0.5 h. Cytoplasmic and nuclear extracts from 500,000 cells were analyzed by Western blotting using anti-p65 and the relative levels of nuclear p65 [N (%)] were calculated after densitometric quantification of chemiluminescence .

Figure 5. Regulation of GCLC/GCLM expression by the IKK β pathway. (A) Antibodies against p65 and p50, c-JUN and control IgG were used for ChIP using chromatin isolated from un-stressed wild type and *Ikk β* (-/-) cells. The precipitates were subjected to PCR amplification using primers for various regions of the *Gclc* and *Gclm* promoters, as indicated in the brackets. The PCR amplified genomic DNA without ChIP was used as total input control. The PCR products were resolved on a gel and photographed. ChIP MAPPER (www.chipmapper.com) analyses showed potential NF- κ B (p50/p65) (green) and AP-1 (orange) binding sites in (B): the -2000 to +1 bp promoter of *Gclc* and (C) the -1500 to +500 promoter of *Gclm*. The ChIP data are fold-changes over IgG control determined by raising 2 to the power of $-\Delta\Delta C_T$ resulting from qRT-PCR (See Supplemental Materials). Statistical analyses were done by comparing the mean values in wild type (black bars) and *Ikk β* (-/-) (grey bars) cells.

MOL #61424

Figure 6. Over-expression of GCLC and GCLM in *Ikkβ* (-/-) cells partially restores GSH levels.

Wild type and *Ikkβ* (-/-) cells were transfected with empty or GCLC and GCLM expression vectors for 24 h. (A) GSH and GSSG levels were measured and redox potentials calculated as in Fig. 1. (B) cells were treated with sodium arsenite (50 μM) for 6 h, followed by CM-H2DCFDA labeling. The nuclei were identified following staining with DAPI (blue) and the ROS-activated DCF fluorescence (green) was observed with fluorescence microscopy. Wild type and/or the *Ikkβ* (-/-) cells transfected with empty or GCLC and GCLM expression vectors were treated with 50 μM sodium arsenite for 6 h. (C) The cells were stained with DAPI and cells with condensed nuclei (i.e. apoptotic cells) were identified under fluorescence microscopy. Numbers represent 3 fields of triplicate samples. Results were the mean values ± S.E. from at least three independent experiments. Statistical analyses were done by comparing the mean values in un-transfected *Ikkβ* (-/-) cells. * $p < 0.05$; ** $p < 0.01$; *** $p < 0.001$ are considered significant. (D) The cells were subjected to Annexin V staining and TUNEL analyses. The number of Annexin V and TUNEL positive cells was counted and the % of apoptosis was calculated based on total cell number.

MOL #61424

Table I. Gene expression of redox cycling enzymes

gene name	symbol	avg int	WT:IKKβ(-)
<u>GSH biosynthesis</u>			
glutamate-cysteine ligase, modifier	<i>Gclm</i>	1726	2.53
glutamate-cysteine ligase, catalytic	<i>Gclc</i>	481	1.52
glutathione synthetase	<i>Gss</i>	287	1.47
<u>GSH redox cycling enzymes</u>			
glutathione reductase 1	<i>Gsr</i>	793	1.41
glutathione peroxidase 1	<i>Gpx1</i>	3462	-1.03
glutathione peroxidase 2	<i>Gpx2</i>	39	1.10
glutathione peroxidase 3	<i>Gpx3</i>	61	1.06
glutathione peroxidase 4	<i>Gpx4</i>	7635	1.03
glutathione peroxidase 5	<i>Gpx5</i>	24	1.12
glutathione peroxidase 6	<i>Gpx6</i>	28	1.19
glutathione peroxidase 7	<i>Gpx7</i>	39	-1.13
Cytochrome p450, 2e1	<i>Cyp2e1</i>	23	1.12

Figure 1

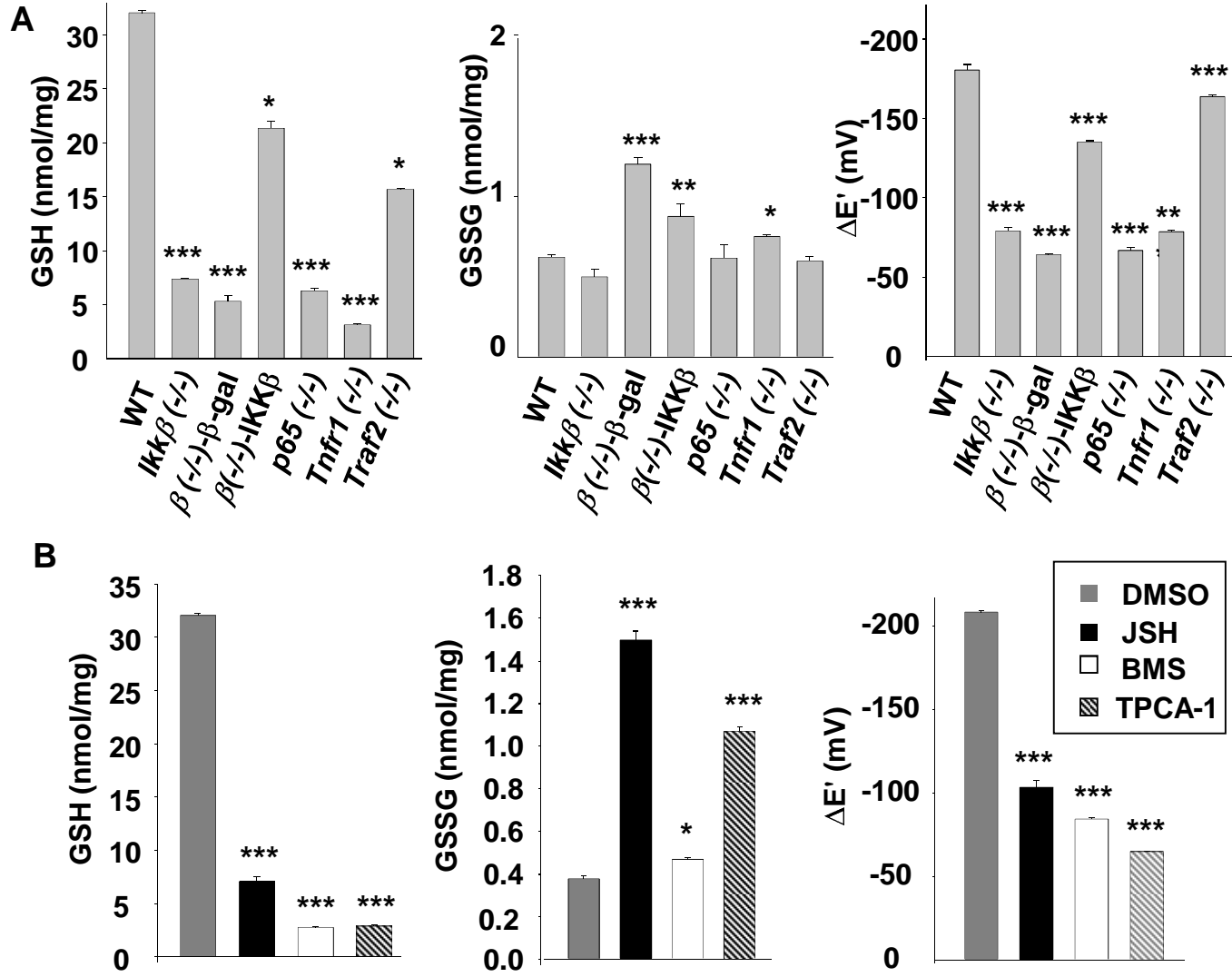


Figure 2

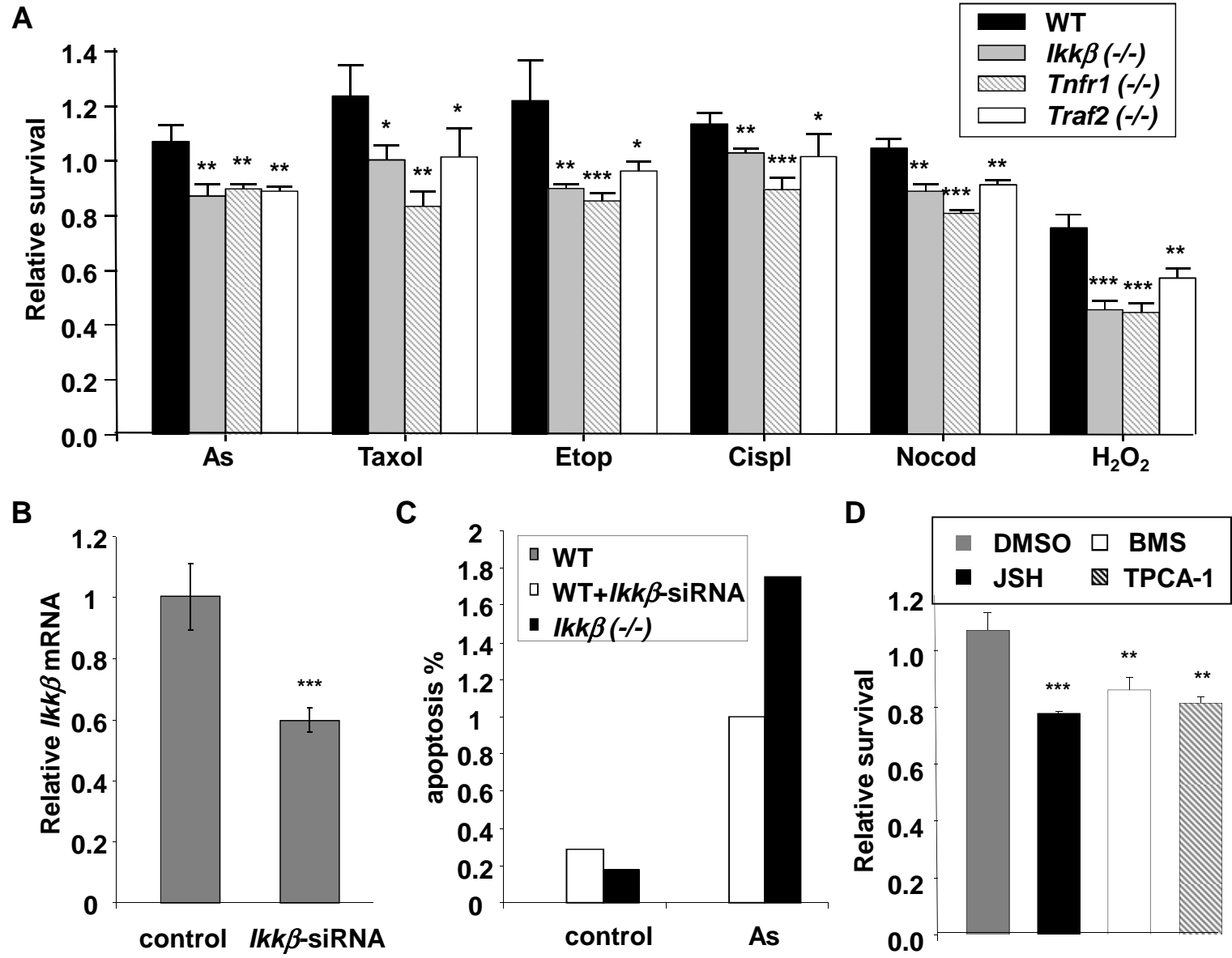


Figure 3

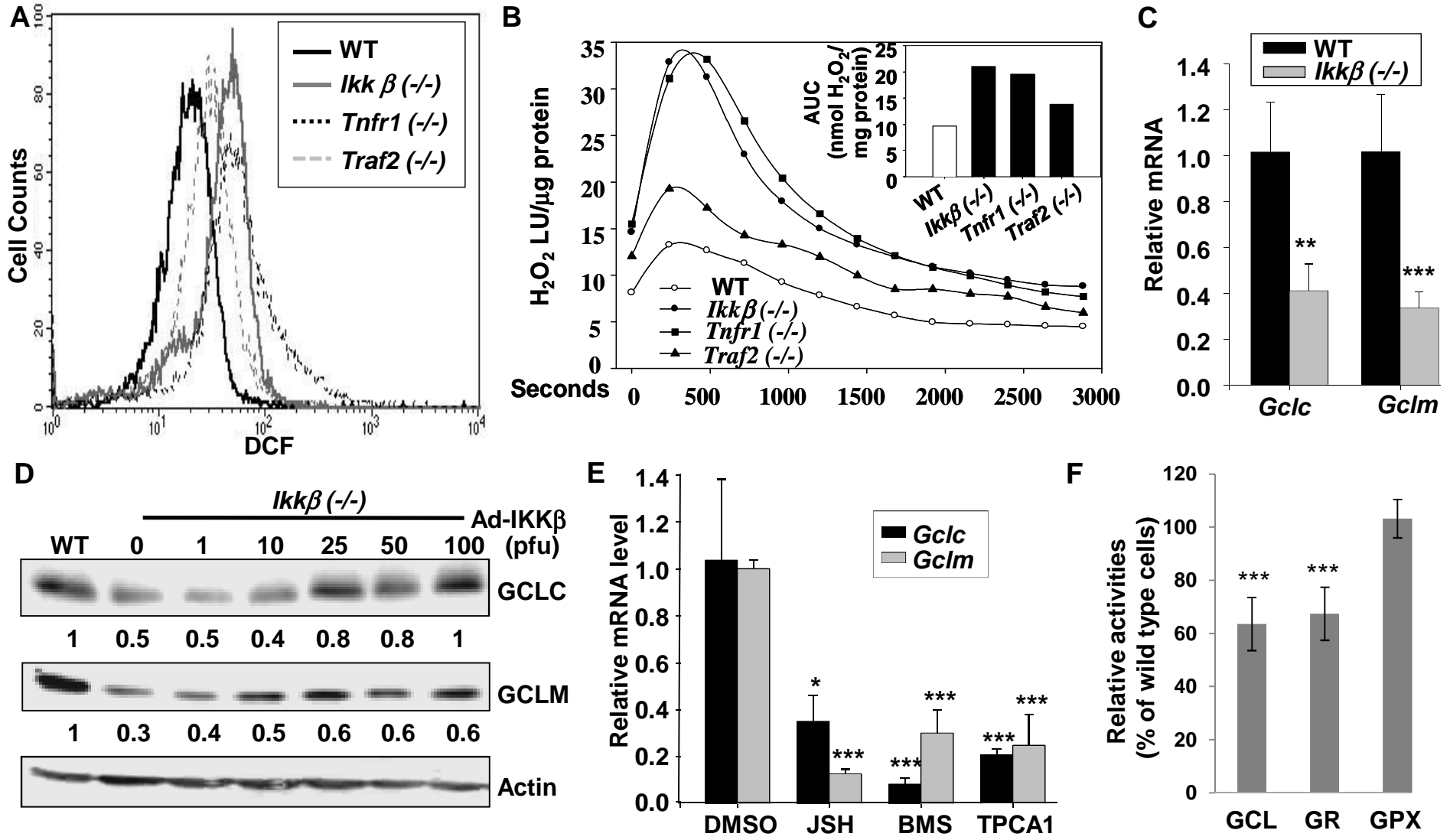


Figure 4

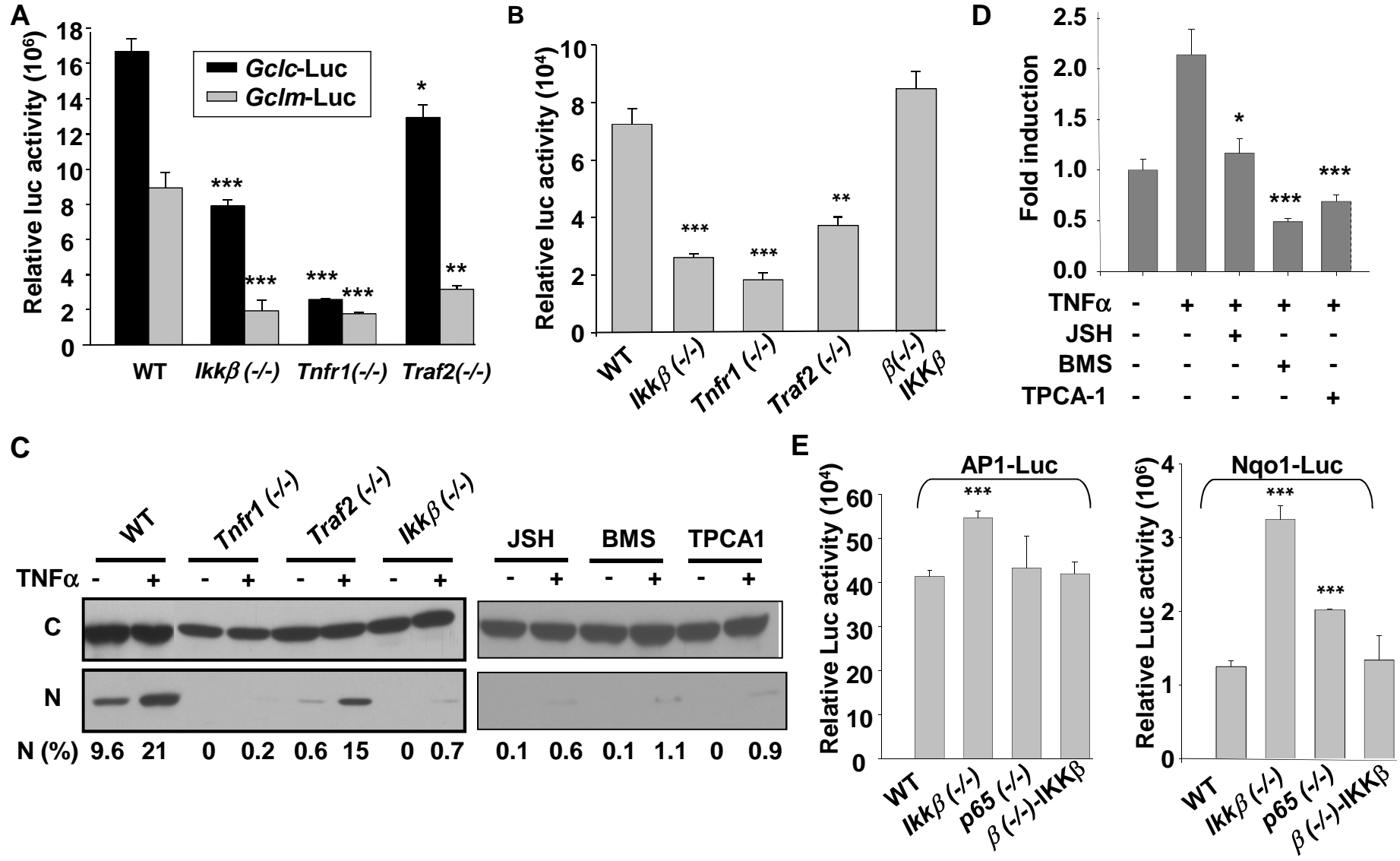
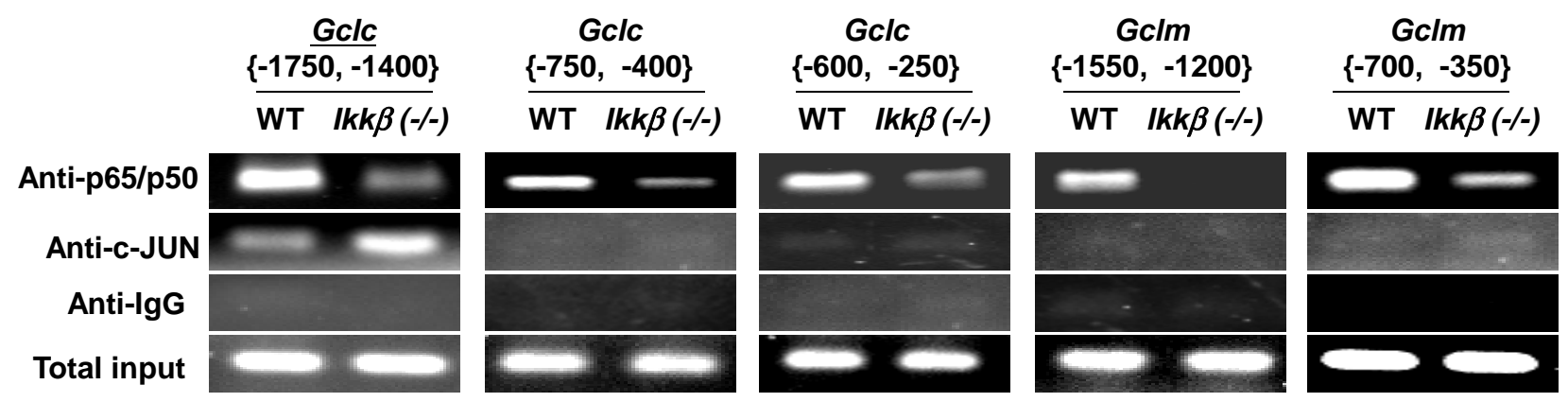
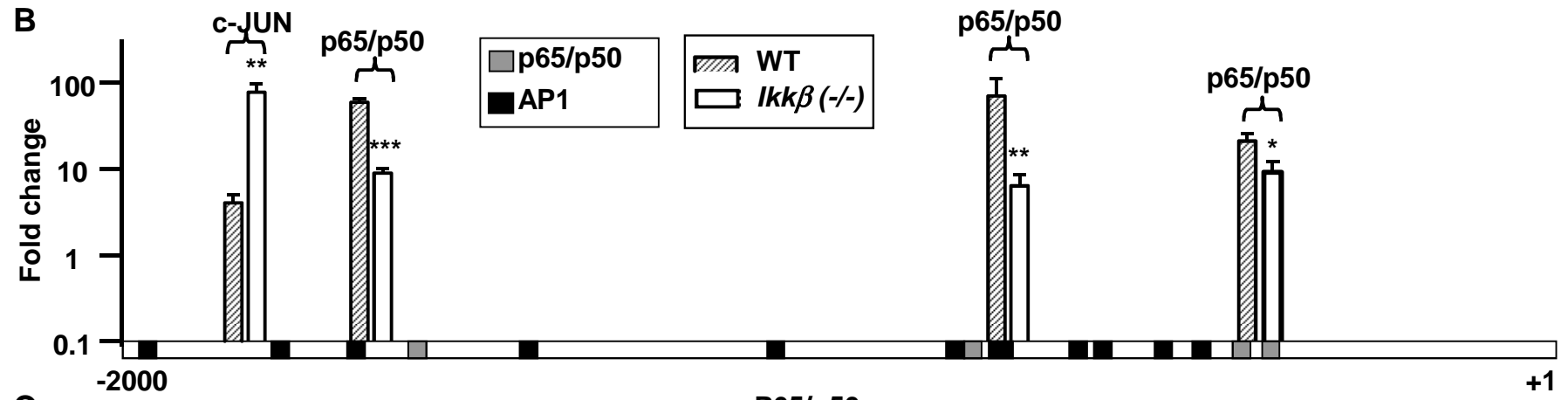


Figure 5

A



B



C

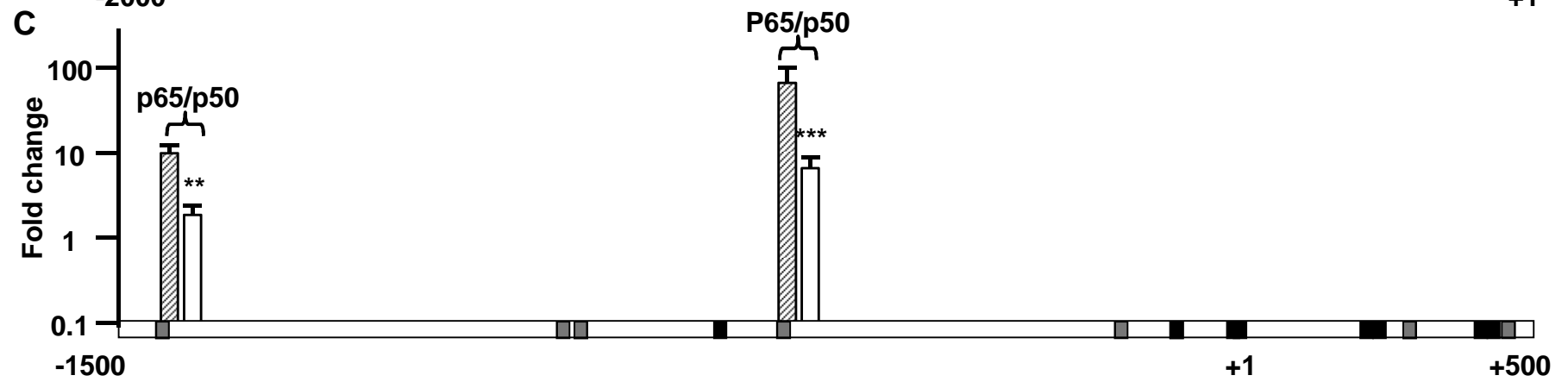


Figure 6

